Available online at www.sciencedirect.com

ScienceDirect

Procedia - Social and Behavioral Sciences 195 (2015) 2242 – 2252

Procedia
Social and Behavioral Sciences

World Conference on Technology, Innovation and Entrepreneurship

Nonlinear Motion Control of a Column Using a Coupled Gyroscope

F. Ünker[a,*], O. Çuvalcı[b]

[a]*Department of Mechanical Engineering, Gümüşhane University ,29100 Gümüşhane, Turkey*
[b]*Department of Mechanical Engineering, Karadeniz Technical University ,61100 Trabzon, Turkey*

Abstract

In this paper, a system of the gyroscopes coupled via the massless torsional springs and the massless torsional dampers mounted on the tip mass of a column subjected to a vibrating base is considered. The coupled gyroscopes are assumed to have reverse angular speeds Ω, and the rotations θ to eliminate the torques due to the springs and the dampers. Taking advantage of the angular momentum of the rotating gyroscope, gyrostabilizer systems are expected to become more widely actualized as they provide an effective means of motion control with several significant advantages for various structures. The non-linear motions of the gyro-column system and the equations of motion for the system are derived following energy (Lagrange) based approaches and examples provided. On the other hand, the effect of the angular velocities of the gyroscopes are studied, and it is shown that the angular velocity (spin velocity) Ω of a gyroscope has a significant effect on the behavior of the dynamic motion. It is also shown how the dampers and springs due to the motion between the suporting gimbals influence the dynamic behavior of the column.

Keywords: Vibration control system, Gyrosope, Gyrostabilizer, Nonlinear Dynamics, Damping

* Corresponding author.Tel.: +90-539-940-6636; fax:+90-456-233-1119.
E-mail addresses: farukunker@gumushane.edu.tr, ocuvalci@ktu.edu.tr

doi:10.1016/j.sbspro.2015.06.309

1. Introduction

Beam carrying a tip mass with (or without) rotary inertia can find application in the modeling of many engineering fields such as tall buildings, towers, piles, antennas, robotic manipulators, appendages of aircrafts, spacecrafts or even vehicles, etc. Hence, there has been a lot of research work on the non-linear dynamics of such beams subject to various boundary and load conditions over the past few decades due to both theoretic and practical demands.

In recent years, several researches have conducted studies investigating the complicated motions which appear in gyrostabilizer, of which there are various types and arrangements, represents one engineering application of the gyroscopic effect, provides an effective means of motion control in many situations; for example, stabilization of bicycles (Beznos, A., Formal'sky, A., Gurfinkel, E., Jicharev, D., Lensky, A., Savitsky,K., and Tchesalin, L., 1998), cars (Schilovski, P., 1909; Schilovski, P., 1914), monorails (Tomlinson, N., 1980), building wind induced vibrations (Higashiyama, H., Yamada, M., Kazao, Y., and Namiki, M., 1998), and boats (Lewis, E., 1989; Perez, T., and Steinmann, P., 2008; Schlick, E., 1904; Sperry, E., 1910). Compared to conventional active mass dampers for wind vibration suppression, gyrostabilizers represent a weight and volume saving. Kitamura, et a1.,(1990) and Nagashima, et al., (1993) have been investigated several types of response control systems for buildings. Consequently this paper considers the coupled gyroscopes are assumed to have reverse angular speeds Ω, and the rotations θ to eliminate the torques on the tip mass due to the torsional springs and the dampers defined by $k\theta$ and $c\dot{\theta}$, respectively. The equations of motion for this gyro-column system are derived following energy (Lagrange) based approaches. Three equations of motion are derived to obtain an understanding of the dynamic behavior of the system. Further, the time evolutions of the nonlinear dynamical system responses are described by numerical simulation. The effect of a gyro's spinning speed Ω is studied, and it is shown that the gyro's spin velocity Ω has a significant effect on the dynamic behavior of the motion.

Table 1. Physical properties of the system

Symbol	*Numerical values*	*Description*
E	210 x 10^9 N/m^2	Young's modulus
h	100 mm	column thickness
b	150 mm	column width
L	5 m	length of the column
ρ	7850 kg/ m^3	density of the column
M_t	2000 kg	tip mass
I_t/M_t	0.2 m^2	ratio of tip mass moment of inertia
I_t	400 kg.m^2	tip mass moment of inertia
I	1.25 x 10^{-5} m^4	geometrical moment of inertia of column
g	9.81 m/s^2	gravitational acceleration
A=b.h	0.015 m^2	area of cross section of column
c	0-200 N.m.s/rad	damping coefficient
k	0-200 N.m/rad	stiffness of torsion spring
$m=m_1=m_2$	50 kg	disk mass of gyroscope
$r=r_1=r_2$	0.2 m	radius of disk
$I_p= I_{p1}= I_{p2} =m.r^2/2$	1 kg.m^2	rotary inertia of disk
$I_o= I_{o1}= I_{o2}=I_p/2$	0.5 kg.m^2	mass moment of inertia of disk
$\Omega=\Omega_1=-\Omega_2$	0-10000 rpm	rotating speed of disk

2. Derivation of Equation of Motion

In this section, to obtain the governing equations of motion of a column-gyro system with a tip mass, The Euler–Bernoulli beam theory was used with small thickness to length ratio. For slender beams (L/h > 20) the effects of shear deformation and rotary inertia of the beam can be neglected. Here, the column has mass density ρ, cross-sectional area A, equivalent Young's modulus E, moment of inertia of plane area I and moment of inertia I_t of a tip mass. Figure 1 shows a column as a vertical cantilever with an end mass M_t to which an additional gyro system is

attached. The horizontal displacement of base subjected to a harmonic base excitation is z. The column is assumed to be initially straight, of length L. The horizontal and vertical elastic displacements at the free end are v and u, respectively. Due to elastic deformation of the column, s represents the distance along arc-length of the column.

The gyro system consists of two disks, which can spin freely about their geometric axis via the massless gimbals mounted to the tip mass of the column. The disk masses, m of the gyro at free end are assumed to have reverse angular speeds Ω, and the rotations θ and also resisted by a torsional spring and damper torque defined by $k\theta$ and $c\dot{\theta}$, respectively as shown in Figure 2.

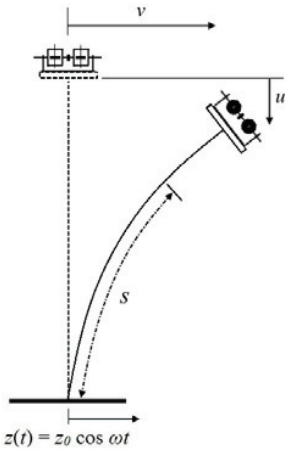

Fig. 1. Cantilever model with end mass, gyroscopes, and base excitation.

The kinetic energy of the gyro-column system as shown in Figure 1 is

$$T = \frac{1}{2}\rho A \int_0^L [(\dot{v}(s,t) + \dot{z}(t))^2 + \dot{u}(s,t)^2]ds + \frac{1}{2}M_t[(\dot{v}(t) + \dot{z}(t))^2 + \dot{u}(t)^2] + \frac{1}{2}I_t\dot{\varphi}^2 + \frac{1}{2}m_1\left[\left(\dot{v}(t) + \dot{z}(t)\right)^2 + \dot{u}(t)^2\right] + \frac{1}{2}m_2\left[\left(\dot{v}(t) + \dot{z}(t)\right)^2 + \dot{u}(t)^2\right] + T_{g1} + T_{g2} \quad (1)$$

where v(t) and u(t) denote the components along the inertial directions of the displacement of the column and the dot denotes derivative with respect to time t.

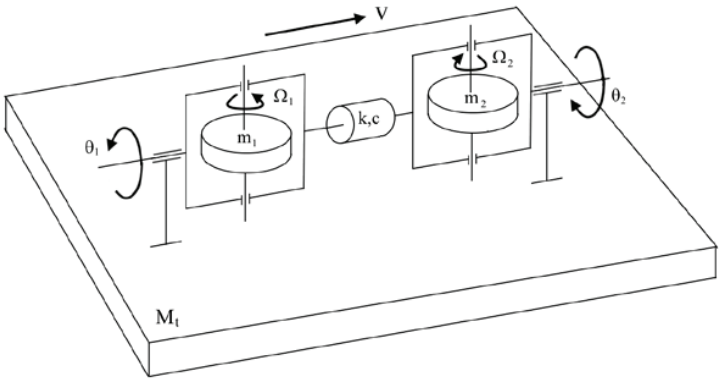

Fig. 2. Coupled gyroscopes via a massless torsional spring with stiffness k and a massless torsional damper with coefficient c.

The motion of a gyro can be described by Euler's angles θ , and φ. It is not difficult to show that the kinetic energy of gyroscopes can be expressed as

$$T_{g1} = \frac{1}{2} I_{01} \left[\dot{\theta_1}^2 + (\dot{\varphi} cos\ \theta_1)^2 \right] + \frac{1}{2} I_{p1} (\Omega_1 + \dot{\varphi} sin\ \theta_1)^2 \tag{2a}$$

$$T_{g2} = \frac{1}{2} I_{02} \left[\dot{\theta_2}^2 + (\dot{\varphi} cos\ \theta_2)^2 \right] + \frac{1}{2} I_{p2} (\Omega_2 + \dot{\varphi} sin\ \theta_2)^2 \tag{2b}$$

The potential energy of the gyro-column system can be written as

$$V = \frac{1}{2} EI \int_0^L q(s,t)^2\, ds - \rho Ag \int_0^L u(s,t)^2\, ds - M_t g u(t) + \frac{1}{2} k(\theta_1 - \theta_2)^2 - m_1 g u(t) - m_2 g u(t) \tag{3}$$

where the orientation angle of the column was given as (Ali and Padhi, 2009; Nayfeh and Pai, 2004; Zavodney and Nayfeh, 1989)

$$q(s,t) = \frac{\partial \varphi}{\partial s} = \varphi' \tag{4}$$

where the prime indicates a partial derivative with respect to position variable s. The angular displacement of the column, φ, can be expressed as

$$\sin \varphi = v' \ \ or \ \cos \varphi = 1 - u' \tag{5}$$

Hence by eliminating terms of order higher than quadratic, yields (Ali and Padhi, 2009; Nayfeh and Pai, 2004)

$$u(s,t) = \frac{1}{2} \int_0^s (v'(\Gamma,t))^2\, d\Gamma \ \ and \ \ u' = 1 - \sqrt{1 - v'^2} \approx \frac{1}{2} v'^2 \ \ and \tag{6}$$

and the equation (5) gives

$$\varphi(s,t) = sin^{-1} v' \approx v' + \frac{1}{6} v'^3 \tag{7}$$

and derivative of this equation can be written as

$$q(s,t) = \varphi' = \frac{v''}{cos\ \varphi} = \frac{v''}{\sqrt{1 - v'^2}} \approx v'' \left(1 + \frac{1}{2} v'^2 \right) \tag{8}$$

Equations (6) to (8) have been expanded resulting equation using a binominal expansion. Since tip mass are significantly larger than the column mass, the column deformation by using the following relationship based on the first mode of the shape function, ψ(s), is (Esmailzadeh and Nakhaie-Jazar, 1998)

$$v(s,t) = v(t)\, \psi(s) \tag{9}$$

$$\psi(s) = \Delta \left(1 - cos \left(\frac{\pi s}{2L} \right) \right) \ and\ \Delta = \frac{1}{\left(1 - cos \left(\frac{\pi s}{2L} \right) \right)} = 1 \text{ for s = L.} \tag{10}$$

Therefore, the kinetic of the system in terms of the transverse displacement at the free end, v, is

$$T = \frac{1}{2}\rho A[\, G_1\dot{v}^2 + 2G_2\dot{v}\dot{z} + \dot{z}^2 L + G_3(v\dot{v})^2] + \frac{1}{2}M_t\left[(\dot{v}+\dot{z})^2 + {G_4}^2(v\dot{v})^2\right] + \frac{1}{2}I_t\left[G_5\dot{v} + \frac{1}{2}{G_5}^3 v^2\dot{v}\right]^2 + \frac{1}{2}m_1\left[(\dot{v}+\dot{z})^2 + {G_4}^2(v\dot{v})^2\right] + \frac{1}{2}m_2\left[(\dot{v}+\dot{z})^2 + {G_4}^2(v\dot{v})^2\right] + T_{g1} + T_{g2} \quad (11)$$

where z is the base displacement of the column. The potential energy of the system in terms of the transverse displacement,v at the free end is

$$V = \frac{1}{2}EI\left[G_6 v^2 + G_7 v^4 + \frac{1}{4}G_8 v^6\right] - \frac{1}{2}G_9\rho A g v^2 - \frac{1}{2}G_4 M_t g v^2 + \frac{1}{2}k(\theta_1-\theta_2)^2 - \frac{1}{2}G_4 m_1 g v^2 - \frac{1}{2}G_4 m_2 g v^2 \quad (12)$$

The dissipation function D takes the form

$$D = \frac{1}{2}c\left(\dot{\theta}_2 - \dot{\theta}_1\right)^2 \quad (13)$$

Using the displacement model in equation (10), the constants from G_1 to G_9 are

$$G_1 = \int_0^L \left(\psi(s)\right)^2 ds,\ G_2 = \int_0^L \psi(s)\, ds, \qquad G_3 = \int_0^L \left(\int_0^s \left(\psi'(\Gamma)\right)^2 d\Gamma\right)^2 ds,\ G_4 = \int_0^L (\psi'(s))^2\, ds,$$
$$G_5 = \psi'(L),\ G_6 = \int_0^L \left(\psi''(s)\right)^2 ds, \qquad G_7 = \int_0^L \left(\psi'(s)\psi''(s)\right)^2 ds,$$
$$G_8 = \int_0^L \left(\psi'(s)\right)^4\left(\psi''(s)\right)^2 ds, \qquad G_9 = \int_0^L \left(\int_0^s \left(\psi'(\Gamma)\right)^2 d\Gamma\right) ds \quad (14)$$

Table 2. Constants of the equation of motion of the gyro-column system in SI units

G_1	G_2	G_3	G_4	G_5	G_6	G_7	G_8	G_9
1.1338	1.8169	0.0552	0.2467	0.3142	0.0244	6.0087e-4	2.9652e-5	0.3669

The equations of motion describing the system can be obtained from the Lagrange equations, for this system become

$$\frac{d}{dt}\left(\frac{\partial T}{\partial \dot{v}}\right) - \frac{\partial T}{\partial v} + \frac{\partial D}{\partial \dot{v}} + \frac{\partial V}{\partial v} = 0, \qquad \frac{d}{dt}\left(\frac{\partial T}{\partial \dot{\theta}_1}\right) - \frac{\partial T}{\partial \theta_1} + \frac{\partial D}{\partial \dot{\theta}_1} + \frac{\partial V}{\partial \theta_1} = 0,$$
$$\frac{d}{dt}\left(\frac{\partial T}{\partial \dot{\theta}_2}\right) - \frac{\partial T}{\partial \theta_2} + \frac{\partial D}{\partial \dot{\theta}_2} + \frac{\partial V}{\partial \theta_2} = 0, \quad (15)$$

2.1. Equations of motion of the column and gyros at the free end

The following differential equation is evaluated based on Eqs. (11-15): the equation of motion of tip mass can be written as

$$\left\{\begin{array}{c}\rho AG_1+m_1+m_2+M_t+I_tG_5{}^2+\left(\rho AG_3+(m_1+m_2+M_t)G_4{}^2+I_tG_5{}^4\right)v^2+\frac{1}{4}I_tG_5{}^6v^4\\+\left(G_5+\frac{1}{2}v^2\,G_5{}^3\right)^2\left[I_{o1}(\cos\theta_1)^2+I_{p1}(\sin\theta_1)^2\right]+\left(G_5+\frac{1}{2}v^2\,G_5{}^3\right)^2\left[I_{o2}(\cos\theta_2)^2+I_{p2}(\sin\theta_2)^2\right]\end{array}\right\}\ddot{v}$$

$$+\left[\rho AG_3+(m_1+m_2+M_t)G_4{}^2+I_tG_5{}^4+\frac{1}{2}I_tG_5{}^6v^2\right]v\dot{v}^2$$

$$+\left[EIG_6-\rho AgG_9-(m_1+m_2+M_t)gG_4+2EIG_7v^2+\frac{3}{4}EIG_8v^4\right]v$$

$$+\left(G_5+\frac{1}{2}v^2\,G_5{}^3\right)\left[\begin{array}{c}\left(I_{p1}-I_{01}\right)\left(\dot{v}G_5+\frac{1}{2}v^2\dot{v}\,G_5{}^3\right)\dot{\theta}_1\,sin\,2\theta_1\\+I_{o1}\left(v\dot{v}^2G_5{}^3\right)(\cos\theta_1)^2\\+I_{p1}\left(v\dot{v}^2G_5{}^3\right)(\sin\theta_1)^2\\+I_{p1}\Omega_1\,\dot{\theta}_1\cos\theta_1\end{array}\right]$$

$$+\left(G_5+\frac{1}{2}v^2\,G_5{}^3\right)\left[\begin{array}{c}\left(I_{p2}-I_{02}\right)\left(\dot{v}G_5+\frac{1}{2}v^2\dot{v}\,G_5{}^3\right)\dot{\theta}_2\,sin\,2\theta_2\\+I_{o2}\left(v\dot{v}^2G_5{}^3\right)(\cos\theta_2)^2\\+I_{p2}\left(v\dot{v}^2G_5{}^3\right)(\sin\theta_2)^2\\+I_{p2}\Omega_2\,\dot{\theta}_2\cos\theta_2\end{array}\right]$$

$$=-(\rho AG_2+m_1+m_2+M_t)\ddot{z} \tag{16}$$

The following differential equation of motion of gyro 1 is obtained.

$$I_{01}\ddot{\theta}_1-\frac{1}{2}\left(I_{p1}-I_{01}\right)\left(\dot{v}G_5+\frac{1}{2}v^2\dot{v}\,G_5{}^3\right)^2 sin\,2\theta_1-I_{p1}\Omega_1\left(\dot{v}G_5+\frac{1}{2}v^2\dot{v}\,G_5{}^3\right)cos\,\theta_1$$
$$-c\left(\dot{\theta}_2-\dot{\theta}_1\right)-k(\theta_2-\theta_1)=0 \tag{17}$$

The following differential equation of motion of gyro 2 is obtained.

$$I_{02}\ddot{\theta}_2-\frac{1}{2}\left(I_{p2}-I_{02}\right)\left(\dot{v}G_5+\frac{1}{2}v^2\dot{v}\,G_5{}^3\right)^2 sin\,2\theta_2-I_{p2}\Omega_2\left(\dot{v}G_5+\frac{1}{2}v^2\dot{v}\,G_5{}^3\right)cos\,\theta_2$$
$$+c\left(\dot{\theta}_2-\dot{\theta}_1\right)+k(\theta_2-\theta_1)=0 \tag{18}$$

3. Numerical Simulations

In the following calculations, a rectangle-cross column is considered with thickness h =100 mm, width b = 150 mm, length L = 5 m, density ρ= 7850 kg/m^3, and Young's modulus along the axial direction E=210 x10^9 N/m^2. Equations may be resolved by using a Matlab software tool that involves the fourth-order Runge-Kutta method. The parameters of the numerical example are given in Table 1. In order to identify the dynamical behavior, the time history is simulated, with the time step size of 0.05 s, and zero initial conditions and frequency response is simulated, with the time step size of 0.05 s, and zero initial conditions.

Figures 3, 5, 7 and 9 represent the frequency response curves of the column and gyro at the free end for the disk velocities of (o) Ω=0 rpm, (+) Ω=5000 rpm and (.) Ω=10000 rpm, respectively. It demonstrates that the displacement responses of the column can be considerably reduced when the disk speed is increased. The gyro reduces the maximum top displacement of column by 90 % by using the disk speed of Ω=10000 rpm. As seen from the figures, the moment of inertia of gyro has the possibility to reduce the vibration by increasing rotating speed Ω of disk.

In the case of the base excitation frequency ω=5.1 rad/s with z=0.05cos(ωt), Figures 4, 6, 8 and 10 show time responses of the column (left) and the gyro response (right) at the free end for the disk speeds of (blue) Ω = 0 rpm,

(red) Ω=5000 rpm, and (green) Ω=10000 rpm, respectively. The case of c=50 N.m.s/rad at k=0 N.m/rad, is shown in Figure 4, which differs from the time responses in Figure 6. It presented that the decreasing stiffness to zero has slightly effect on reducing the vibration of column but can result in the transient dynamics at Ω=5000 rpm as shown in Figure 4. When damping coefficient is decreased to zero, the moment of inertia of gyro system has no possibility to reduce the vibration of column as shown in Figure 10. Optimum damping coefficient is preferred as increasing coefficient to 200 N.m.s/rad can cause increasing displacement of column at free end as shown in Figure 8 compared to Figure 6 at Ω=10000 rpm.

As seen from the figures, by changing the coefficients of spring and damper, the moment of inertia of gyro system has the possibility to reduce the vibration of column. But, compared to the time responses of gyro, the precession angle, θ of gyro system can be increased by changing the coefficients of spring and damper if disk has the lower rotating speed Ω of disk. The time histories have also the unstable responses by decreasing rotating speed Ω of disk. However, the time histories can be improved via optimum coefficients of spring and damper.

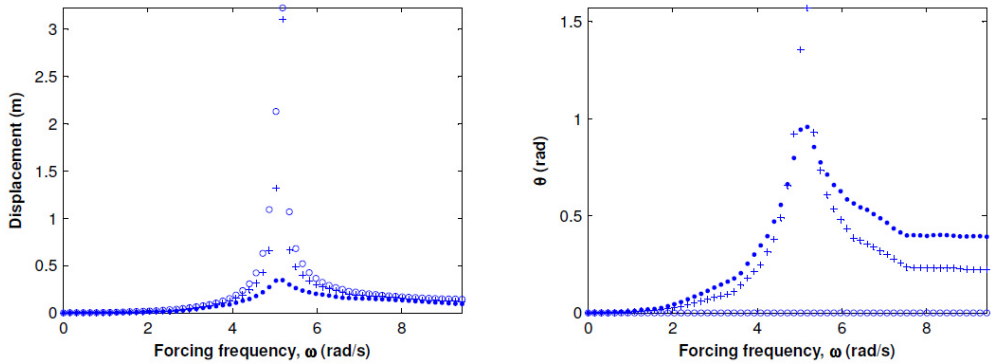

Fig. 3. Frequency response curves for c=50 N.m.s/rad and k=0 N.m/rad: **(left)** tip response of column, **(right)** gyro response for **(o)** Ω=0 rpm, **(+)** Ω=5000 rpm, and **(.)** Ω = 10000 rpm with the base excitation of z=0.05cos(ωt).

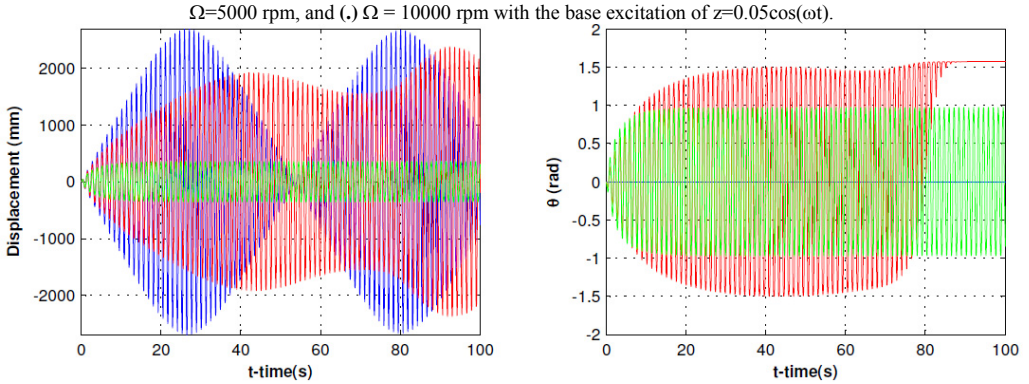

Fig. 4. Time response of the column **(left)** and the gyro system **(right)** at the free end with c=50 N.m.s/rad and k=0 N.m/rad for **(blue)** Ω = 0 rpm, **(red)** Ω=5000 rpm, and **(green)** Ω=10000 rpm in the case of the base excitation frequency ω=5.1 rad/s with z=0.05cos(ωt).

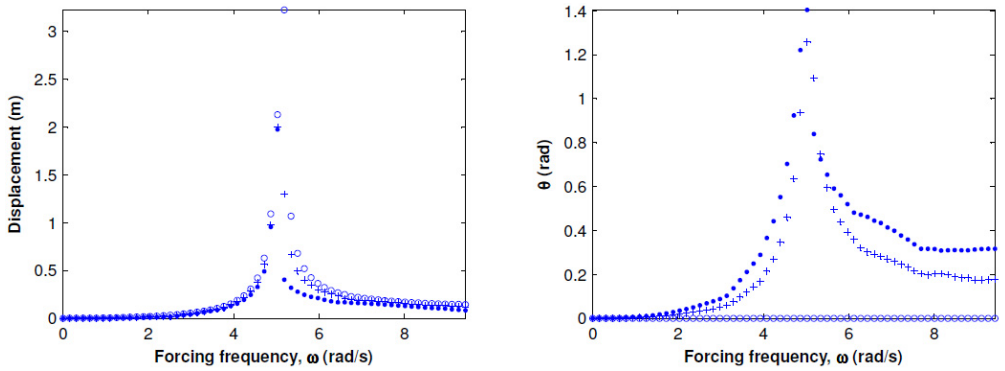

Fig. 5. Frequency response curves for c=50 N.m.s/rad and k=200 N.m/rad: **(left)** tip response of column, **(right)** gyro response for **(o)** Ω=0 rpm, **(+)** Ω=5000 rpm, and **(.)** Ω = 10000 rpm with the base excitation of z=0.05cos(ωt).

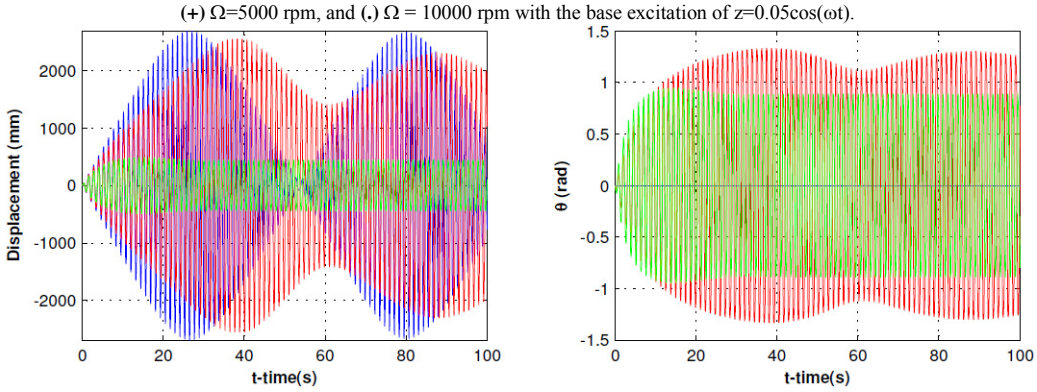

Fig. 6. Time response of the column **(left)** and the gyro system **(right)** at the free end with c=50 N.m.s/rad and k=200 N.m/rad for **(blue)** Ω = 0 rpm, **(red)** Ω=5000 rpm, and **(green)** Ω=10000 rpm in the case of the base excitation frequency ω=5.1 rad/s with z=0.05cos(ωt).

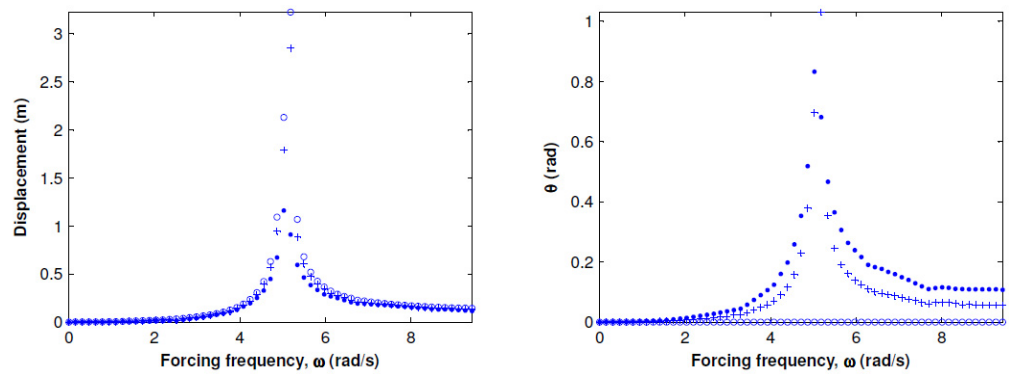

Fig. 7. Frequency response curves for c=200 N.m.s/rad and k=200 N.m/rad: **(left)** tip response of column, **(right)** gyro response for **(o)** Ω=0 rpm, **(+)** Ω=5000 rpm, and **(.)** Ω = 10000 rpm with the base excitation of z=0.05cos(ωt).

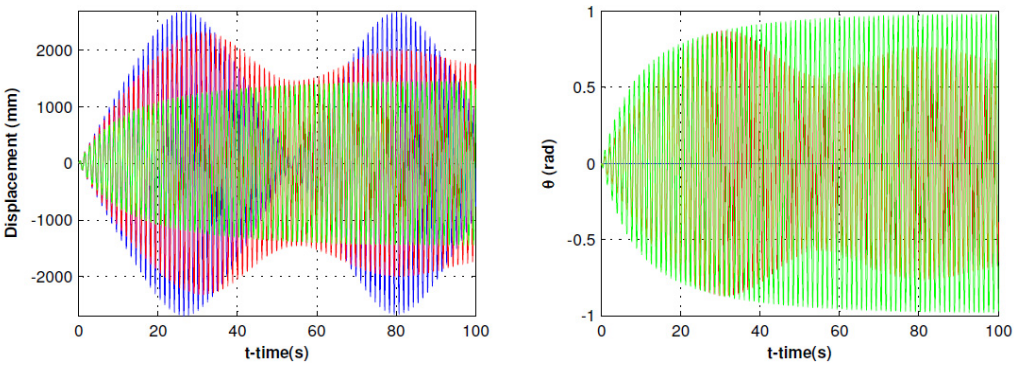

Fig. 8. Time response of the column **(left)** and the gyro system **(right)** at the free end with c=200 N.m.s/rad and k=200 N.m/rad for **(blue)** Ω = 0 rpm, **(red)** Ω=5000 rpm, and **(green)** Ω=10000 rpm in the case of the base excitation frequency ω=5.1 rad/s with z=0.05cos(ωt).

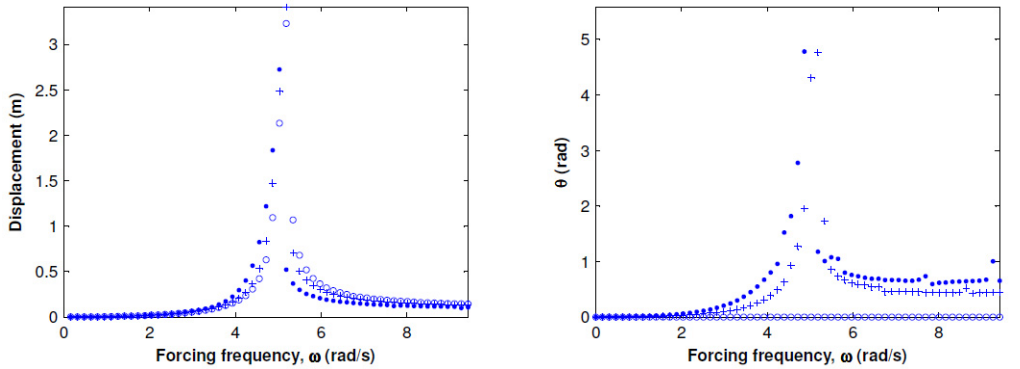

Fig. 9. Frequency response curves for c=0 N.m.s/rad and k=200 N.m/rad: **(left)** tip response of column, **(right)** gyro response for **(o)** Ω=0 rpm, **(+)** Ω=5000 rpm, and **(.)** Ω = 10000 rpm with the base excitation of z=0.05cos(ωt).

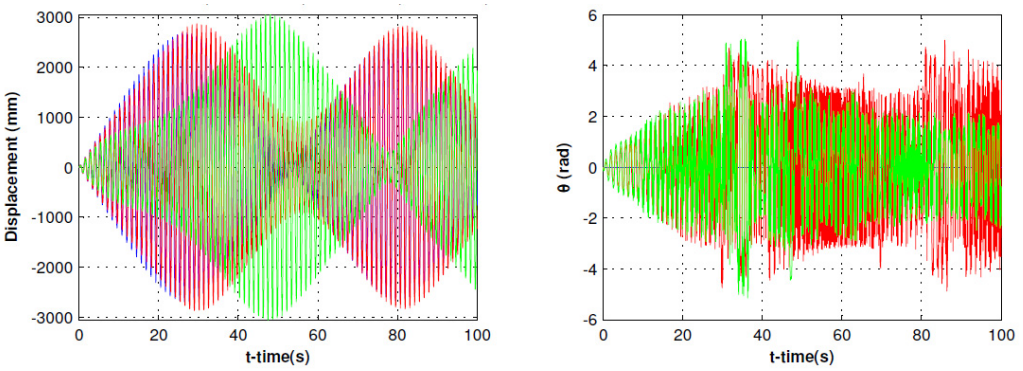

Fig.10. Time response of the column **(left)** and the gyro system **(right)** at the free end with c=0 N.m.s/rad and k=200 N.m/rad for **(blue)** Ω = 0 rpm, **(red)** Ω=5000 rpm, and **(green)** Ω=10000 rpm in the case of the base excitation frequency ω=5.1 rad/s with z=0.05cos(ωt).

4. Conclusions

In this research, the design method involves the technique to couple the dynamic equation of a gyro resisted by torsional spring and damping torque defined by $k\theta$ and $c\dot{\theta}$, respectively. The coupled gyroscopes are assumed to have reverse angular speeds Ω, and the rotations θ to eliminate the torques on the tip mass due to the torsional springs and the dampers. From the coupled dynamic equations, the design rules were obtained for a gyro as a vibration absorber, which can be realized by adjusting spring and damping coefficients. Throughout the entire analysis physical properties in Table1 have been considered to be constant in the system. The following conclusions are drawn from the results of the present study:

- The moment of inertia of gyro-system has the possibility to reduce the vibration by increasing rotating speed Ω of disk. The performance of the gyro in the system is found to recover at high angular speeds as far as frequency response of the gyro at the column is concerned.

- Strong correlation between simulated angular speed and damping coefficient. Optimum damping coefficient is preferred as increasing coefficient can cause increasing displacement of column at free end.

- The displacement rate strongly depends on damping coefficient of gyro system and it also depends on spring coefficient. The study clearly indicates that displacement is also influenced with the coefficient of spring. Therefore the cooperation of the spring with the disk speed is not negligible and the spring coefficient should always be considered in such calculations. If disk has the lower rotating speed, the transient dynamics of the precession angle, θ of gyro-system can be improved by optimizing the coefficients of spring as has also been shown via numerical simulations.

- From the numerical analysis it has become clear that increasing the rotating speed Ω of the disk, the time response is decreased. But increase in rotating speed of the disk is limited due to design of gyro system as well as from economical point of view. Time response can be improved by optimizing the coefficients of damper and spring, but the improvement is still limited with the rotating speed Ω.

Acknowledgments

This study was mainly supported by the Scientific and Technological Research Council of Turkey (TUBITAK) under Grant no: 114M760.

References

Ali, S. F., & Padhi, R. (2009). Active vibration suppression of non-linear beams using optimal dynamic inversion. Proceedings of the Institution of Mechanical Engineers Part I. *Journal of Systems and Control Engineering, 223,* 657–672.

Beznos, A., Formal'sky, A., Gurfinkel, E., Jicharev, D., Lensky, A., Savitsky, K., & Tchesalin, L. (1998). Control of autonomous motion of two-wheel bicycle with gyroscopic stabilization. *Proceedings of the IEEE International Conference on Robotics and Automation, 3,* 2670–2675.

Esmailzadeh, E., & Nakhaie-Jazar, G. (1998). Periodic behavior of a cantilever beam with end mass subjected to harmonic base excitation. *International Journal of Non-Linear Mechanics, 33(4),* 567–577.

Higashiyama, H., Yamada, M., Kazao, Y., & Namiki, M. (1998). Characteristics of active vibration control system using gyro-stabilizer. *Eng. Struct., 20(3),* 176–183.

Kitamura, H., Kawamura, S., Yamada, M., & Fujii, S. (1990). Structural response control technologies of Taisei corporation. *Proc.ofthe U.S.National Workshop on Structural Control Research,* 141-150.

Lewis, E. (1989). *Principles of Naval Architecture*. The Society of Naval Architects and Marine Engineers, New York.

Nagasima, I., Yamada, M., & Tujita, O. (1993). Development and full scale implement of passive and active response control systems to buildings. *International Workshop on Structural Control*, 333-345.

Nayfeh, A., & Pai, P. (2004). *Linear and Nonlinear Structural Mechanics.* New Jersey, Wiley Interscience.

Perez, T., & Steinmann, P. (2008). Advances in gyrostabilisation of vessel roll motion, Proceedings of Pacific International Maritime Conference, Sydney, NSW.

Sperry, E. (1910). The gyroscope for marine purposes. *Soc. Nav. Archit. Mar. Eng., Trans*., *18,* 143–154.

Schlick, E. (1904). The gyroscopic effect of flywheels on board ship. *Transactions of the Institute of Naval Architects*, *23,* 117–134.

Schilovski, P. (1909). Gyrocar, Patent No. GB 12,021.

Schilovski, P. (1914). Gyrocar, Patent No. GB 12,940.

Tomlinson, N. (1980). *Louis Brennan Inventor Extraordinaire*, John Halliwell, Chatham.

Zavodney, L., & Nayfeh, A. (1989). The nonlinear response of a slender beam carrying a lumped mass to a principal parametric excitation: Theory and experiment. *International Journal of Non-Linear Mechanics, 24(2),* 105–125.